Received: 9 May 2019 | Revised: 4 November 2019 | Accepted: 19 November 2019

DOI: 10.1002/ptr.6584

RESEARCH ARTICLE

WILEY

Rosmarinic acid reverses non-small cell lung cancer cisplatin resistance by activating the MAPK signaling pathway

Xiao-Zhong Liao[1,2] | Ying Gao[2] | Ling-Ling Sun[1] | Jia-Hui Liu[2] | Han-Rui Chen[1] | Ling Yu[1] | Zhuang-Zhong Chen[1] | Wen-Hui Chen[3] | Li-Zhu Lin[1]

[1]Department of Oncology, the First Affiliated Hospital, Guangzhou University of Chinese Medicine, Guangzhou, China

[2]Department of Oncology, the First Affiliated Hospital, Sun Yat-sen University, Guangzhou, China

[3]Department of Oncology, the First Affiliated Hospital, Jinan University, Guangzhou, China

Correspondence
Li-Zhu Lin, Department of Oncology, the First Affiliated Hospital, Guangzhou University of Chinese Medicine, Yard 16, Airport Road, Guangzhou 510405, China.
Email: lizhulin26@yahoo.com;
Wen-Hui Chen, Department of Oncology, the First Affiliated Hospital, Jinan University, Guangzhou 510630, China.
Email: wenhuichen221@126.com

Funding information
National Natural Science Foundation of China, Grant/Award Number: 81573780; Natural Science Foundation of Guangdong Province, Grant/Award Number: 2018B030311023

Cisplatin (DDP) is one of the first-line chemotherapeutic agents for non-small cell lung cancer (NSCLC). However, repeated use of cisplatin in clinical practice often induces chemoresistance. The aims of this study were to investigate whether rosmarinic acid (RA) could reverse multidrug resistance (MDR) in NSCLC and to explore the underlying mechanisms. Our data demonstrated that RA significantly inhibited NSCLC cell proliferation and cell colony formation in a dose-dependent manner, induced G1 phase cell cycle arrest and apoptosis, and increased the sensitivity of cell lines resistant to DDP. Mechanistically, RA inhibited NSCLC cell growth, arrested cell cycle, and induced apoptosis by activating MAPK and inhibiting the expression of P-gp and MDR1, which correspondingly enhanced p21 and p53 expression. We observed that the growth of xenograft tumors derived from NSCLC cell lines in nude mice was significantly inhibited by combination therapy. We demonstrate that RA is a potentially effective MDR reversal agent for NSCLC, based on downregulation of MDR1 mRNA expression and P-gp. Together, these results emphasize the putative role of RA as a resistance reversal agent in NSCLC.

KEYWORDS
cisplatin, MAPK, multidrug resistance, non-small cell lung cancer, rosmarinic acid

1 | INTRODUCTION

Lung cancer is the most frequent cause of cancer-related death worldwide (Ferlay et al., 2015), and more than 80% of all lung cancer cases are diagnosed as non-small cell lung cancer (NSCLC; Reck et al., 2014). DDP is one of the first-line chemotherapeutic agents for NSCLC (Fennell et al., 2016). However, repeated use of DDP in clinical practice often induces chemoresistance in tumor cells, allowing them to avoid the apoptosis induced by DDP treatment (Rosell, Lord, Taron, & Reguart, 2002). Moreover, once a tumor cell becomes resistant to an antitumor drug, the cell might also be given the ability to resist other antitumor drugs with different structures, which is referred to as multidrug resistance (MDR; Rosell et al., 2002; Schneider, Paul, Ivy, & Cowan, 1999). Therefore, it is urgent to explore the molecular mechanism of DDP resistance and adopt effective drug combinations to weaken chemotherapy resistance in NSCLC.

One known obvious cause of MDR is high expression of ATP-binding cassette (ABC) transporters on the plasma membrane of cancer cells (Chen et al., 2016). ABC transporters mediate energy-dependent drug efflux and can significantly reduce the success rate of cancer treatment (Gottesman & Pastan, 2015). P-glycoprotein (P-gp), which is affiliated with the ABC superfamily, is strongly linked to

Abbreviations: 2D, two-dimensional; CCK8, cell counting kit-8; CI, combination index; CID, compound ID; DDP, cisplatin; ECL, electrochemiluminescence system; Fa, fraction affected; FCM, flow cytometry; HRP, horseradish peroxidase; NSCLC, non-small cell lung cancer; PI, propidium iodide; PI3K, phosphatidylinositol 3-kinase; PVDF, polyvinylidene difluoride; RA, rosmarinic acid; TCM, traditional Chinese medicine.

Xiao-Zhong Liao and Ying Gao contributed equally to this work.

MDR due to its role in drug efflux, which reduces the therapeutic effect of drugs (Alakhova & Kabanov, 2014; Pluchino, Hall, Goldsborough, Callaghan, & Gottesman, 2012). An effective method to reverse P-gp-mediated MDR is using its inhibitors to reduce efflux of chemotherapeutic agents and increase the sensitivity of tumor cells to chemotherapeutic drugs (Choi & Yu, 2014; Zhou et al., 2008). Therefore, finding and developing chemosensitizers is vital for reversing MDR. Although some compounds have been identified as candidate agents for MDR reversal, most of them exhibit pronounced toxic side effects, limiting their clinical application (Abdallah, Al-Abd, El-Dine, & El-Halawany, 2015). Compounds derived from natural sources have become the new trend in P-gp inhibitor discovery because they have less toxicity and greater effects (Xia et al., 2012).

Rosmarinic acid (RA) is a polyphenolic hydroxyl compound isolated from the rosemary plant in the Lamiaceae family (Gutierrez-Grijalva et al., 2017). RA has a variety of promising biological effects, including antimicrobial (Kim, Park, Jin, & Park, 2015), anti-anaphylaxis, anti-inflammatory (Rocha et al., 2015), antioxidant (Zhu et al., 2014), and anticancer (Han et al., 2015) effects. Furthermore, RA could reverse the MDR in SGC7901/Adr cell (F. R. Li et al., 2013). However, the effect of RA on chemoresistance has not been previously investigated and thus remains largely unknown.

In this study, we investigated the effects of RA combined with DDP on cell viability and apoptosis and explored the mechanisms underlying the potential ability of RA to reverse MDR in vitro and in vivo.

2 | METHODS AND MATERIALS

2.1 | Cell lines, culture conditions, and reagents

A549 cells were purchased from Shanghai Institutes for Biological Sciences, Chinese Academy of Sciences (Shanghai, China). A549DDP cells were derived from A549 cells. The two cell lines were cultured in RPMI-1640 culture medium with 10% fetal bovine serum and 100 U/ml penicillin/streptomycin at 37°C in a humidified atmosphere of 5% CO_2. To maintain resistance, 1 μg/ml DDP was added to A549DDP cell cultures. When the cells reached confluency, they were harvested and plated for either subsequent passages or drug treatments. RA was dissolved in dimethyl sulfoxide to produce a 1 mM stock solution and stored at −20°C for future use. DDP and SP600125 were dissolved in physiological saline to produce a 10 mM stock solution and stored at −20°C for future use.

2.2 | Cell viability assay

Cell viability was assessed with a cell counting kit-8 (CCK8) assay. Exponentially growing cells were plated in 96-well culture plates (~6,000/well in 100 μl medium), cultured overnight, and incubated with a series of RA (0–200 μg/ml) or DDP (0–80 μg/ml) concentrations for 48 hr. After addition of 10 μl CCK8 solution per well, the plates were incubated at 37°C for 2 hr, and then, the absorbance (A) was measured at a wavelength of 450 nm on a microculture plate reader (Thermo Scientific, Rockford, IL). The inhibition ratio was calculated as follows: $(A_{control} - A_{treated})/A_{control} \times 100\%$, where $A_{treated}$ and $A_{control}$ are the absorbance of the treated and control cells after 48 hr of incubation, respectively.

2.3 | Calculation of the combination effect index

We determined the inhibitory effects of RA and DDP using CCK8 assays. We used the combination index (CI) described by Chou and Talalay for analysis and performed the analysis by applying the CalcuSyn software. CI < 1 indicates synergism; CI = 1 indicates summation; CI > 1 indicates antagonism.

2.4 | Colony formation assay

Cells were trypsinized to form single cell suspensions and seeded in six-well plates at a density of 800/well. After 10 days of culture, colonies were fixed with methyl alcohol and stained with crystal violet, and then, the clone formation ratio was calculated.

2.5 | Cell cycle analysis

A Cell Cycle Detection Kit purchased from 4A Biotech Co., Ltd. was used to determine the cell cycle distribution. Cells were exposed to RA or DDP alone or in combination for 48 hr, harvested in cold phosphate-buffered saline, fixed in 70% ethanol, and stored overnight at 4°C. The cells were then washed again with cold PBS and incubated with 100 μl RNase in a 37°C water bath for 30 min, followed by labeling with 400 μl propidium iodide (PI) and incubation for 30 min at room temperature in the dark. For each detection, at least 50,000 cells were evaluated. An ACEC NovoCyte flow cytometer equipped with Novoexpress (Becton Dickinson, San Jose, CA) was used to detect the cell cycle distribution.

2.6 | Apoptosis assay

An Annexin-V-FITC apoptosis detection kit purchased from 4A Biotech Co., Ltd. was applied to detect cell apoptosis. Cells were exposed to RA or DDP alone or in combination for 48 hr, harvested in cold phosphate-buffered saline, resuspended in 500 μl incubation buffer containing Annexin-V-FITC and PI, incubated in the dark for 30 min, and analyzed with the ACEC NovoCyte flow cytometer equipped with Novoexpress.

2.7 | Potential target recognition based on PharmMapper

PharmMapper (http://lilab.ecust.edu.cn/pharmmapper/index.php) is supported by a large, in-house repertoire of a pharmacophore database extracted from all the targets in TargetBank, DrugBank,

BindingDB, and PDTD. More than 7,000 receptor-based pharmacophore models (covering information related to 1,627 drug targets, 459 of which are human protein targets) are stored and accessed by PharmMapper. First, the SDF of RA was downloaded from PubChem Compound (https://www.ncbi.nlm.nih.gov/pccompound/) and then uploaded to PharmMapper. Following proper parameter setting, target identification was then carried out, and information regarding the top 300 potential protein targets was obtained.

2.8 | KEGG pathway analysis

Based on KEGG Mapper (https://www.kegg.jp/kegg/tool/map_pathway2.html), the Search&Color Pathway is an advanced version of the KEGG pathway mapping tool, where given objects (genes, proteins, compounds, glycans, reactions, drugs, etc.) are searched against KEGG pathway maps and discovered objects. First, *Homo sapiens* were selected, and then, the top 300 potential protein targets were uploaded; the information associated with the top 100 potential pathways was obtained. A parameter enrichment gene count ≥2 and hypergeometric test significance threshold *p* value of <.05 were used.

2.9 | Western blotting

Cell were treated with RA and DDP for 48 hr, harvested, washed twice in ice-cold PBS, and lysed in sodium dodecyl sulfate (SDS) lysis buffer (SDS: phenylmethylsulfonyl fluoride = 50:1) at 100°C for 20 min. Lysates were centrifuged (12,000 rpm) at 4°C for 15 min, and the supernatant was collected. Equal amounts of lysate (20–30 μg) were denatured in 5× SDS sample buffer, resolved via 12% SDS-polyacrylamide gel electrophoresis, transferred to polyvinylidene difluoride membranes (Millipore), blocked with 5% skimmed milk in Tris-buffered saline containing 0.1% Tween-20 (TBST) at room temperature for 1 hr, and probed with primary antibody (1:1,000) overnight at 4°C. The membranes were incubated with secondary antibody (1:5,000) for 1 hr at room temperature. Protein bands were visualized using an enhanced chemiluminescence kit (Beyotime, Shanghai, China) and imaged via autoradiography. Immunoblotting was performed for Cyclin D1, p21, p53, Caspase-3, cleaved Caspase-3, MDR1/ABCB1 (P-gp), c-Jun N-terminal kinase (JNK), phospho-JNK (p-JNK), Bcl-2, and Bax, and GAPDH served as the loading control.

2.10 | Quantitative real-time RT-PCR (qRT-PCR)

Total RNA was extracted using Trizol reagent (Tiangen, Beijing, China). All RNA samples were measured via spectrophotometry and were reverse-transcribed into cDNA using PrimerScript Master mix (Takara Biotechnology, China) according to the manufacturer's protocol. The mRNA level was evaluated via qRT-PCR with SsoAdvanced Universal SYBR Green Supermix (Bio-Rad, Hercules, CA) and was analyzed with a C1000 Thermal Cycler (CFX96 Real-Time System, Bio-Rad). Each sample was analyzed in triplicate. Relative mRNA levels were calculated using the comparative threshold cycle (CT), with the analyzed gene expression levels normalized to those of GAPDH. Forty cycles (95°C for 3 min, 95°C for 5 s, 59°C for 5 s) were performed on the Light Cycler in a 10-μl reaction volume, followed by generation of a melting curve. The relative changes in gene expression were calculated using the $2^{-\Delta\Delta Ct}$ method, where $\Delta\Delta Ct = \Delta Ct$ (drug treated) $- \Delta Ct$ (control) for RNA samples. The gene-specific primer pairs used in this study were as follows: MDR1, (forward) 5′-CTGCTTGATGG CAAAGAAATAAAG-3′ and (reverse) 5′-GGCTGTTGTCTCCATAGGCAAT-3′; GAPDH, (forward) 5′-GAGTC AACGGATTTGGTCGT-3′ and (reverse) 5′-GAC AAGCTTCCCGTTCTCAG-3′.

2.11 | Xenograft tumor assay in nude mice

Nude female BALB/c-nu/nu mice (4–6 weeks) were purchased from the Institute of Laboratory Animal Sciences, Chinese Academy of Medical Sciences in Beijing, China, and housed in a specific pathogen-free environment. A549 (3×10^6) and A549DDP (3×10^6) cells were injected subcutaneously (s.c.) into the flanks of the mice. When tumors grew to ~6 mm in diameter, the mice were sorted into eight groups (six mice per group). The in vivo treatment protocol with various concentrations of RA or DDP is shown in Figure 6a. The eight groups were treated with vehicle control or RA through intraperitoneal (i.p.) injection every day, and DDP was administered once every 5 days. The volume of administration was 10 μl/g. Tumor volumes were measured at the start of the treatment and every 4 days during the course of the therapy. The tumor length (*L*) and width (*W*) were measured, and the tumor volume (*V*) was calculated as follows: $V = ½ \times L \times W^2$. Tumors were resected on the second day following the last injection and weighed. All experiments were performed in accordance with national ethical guidelines and with approval from the Institutional Animal Care and Use Committee of Sun Yat-sen University.

3 | STATISTICAL ANALYSIS

The data are presented as the means ± *SD* of triplicate samples in at least three independent experiments. Differences between the mean values were analyzed using two-sample Student's *t*-test and one-way analysis of variance; *p*-values below .05 were considered to indicate statistical significance.

4 | RESULTS

4.1 | RA increased the sensitivity of NSCLC cells to cisplatin

First, we constructed a cisplatin-resistant cell line from the NSCLC cell line A549, and named it A549DDP. Then, the cellular morphology of

A549 and A549DDP cells was studied, and we found that the morphology of A549DDP cells was irregular and misaligned, whereas that of A549 cells was fusiform and in alignment. In addition, the cell volume of A549DDP cells was increased compared with that of A549 cells (Figure 1a,b). To verify the resistance of the A549DDP cell line, we performed a CCK8 assay after treatment with DDP for 48 hr. Our data showed that the resistance index value of A549DDP cells was 11.19 ± 0.50 (Figure S1A,B). To evaluate the effect of RA on the viability of A549 and A549DDP cells, a CCK8 assay was performed 48 hr after treatment. As shown in Figure 1c,d, RA significantly

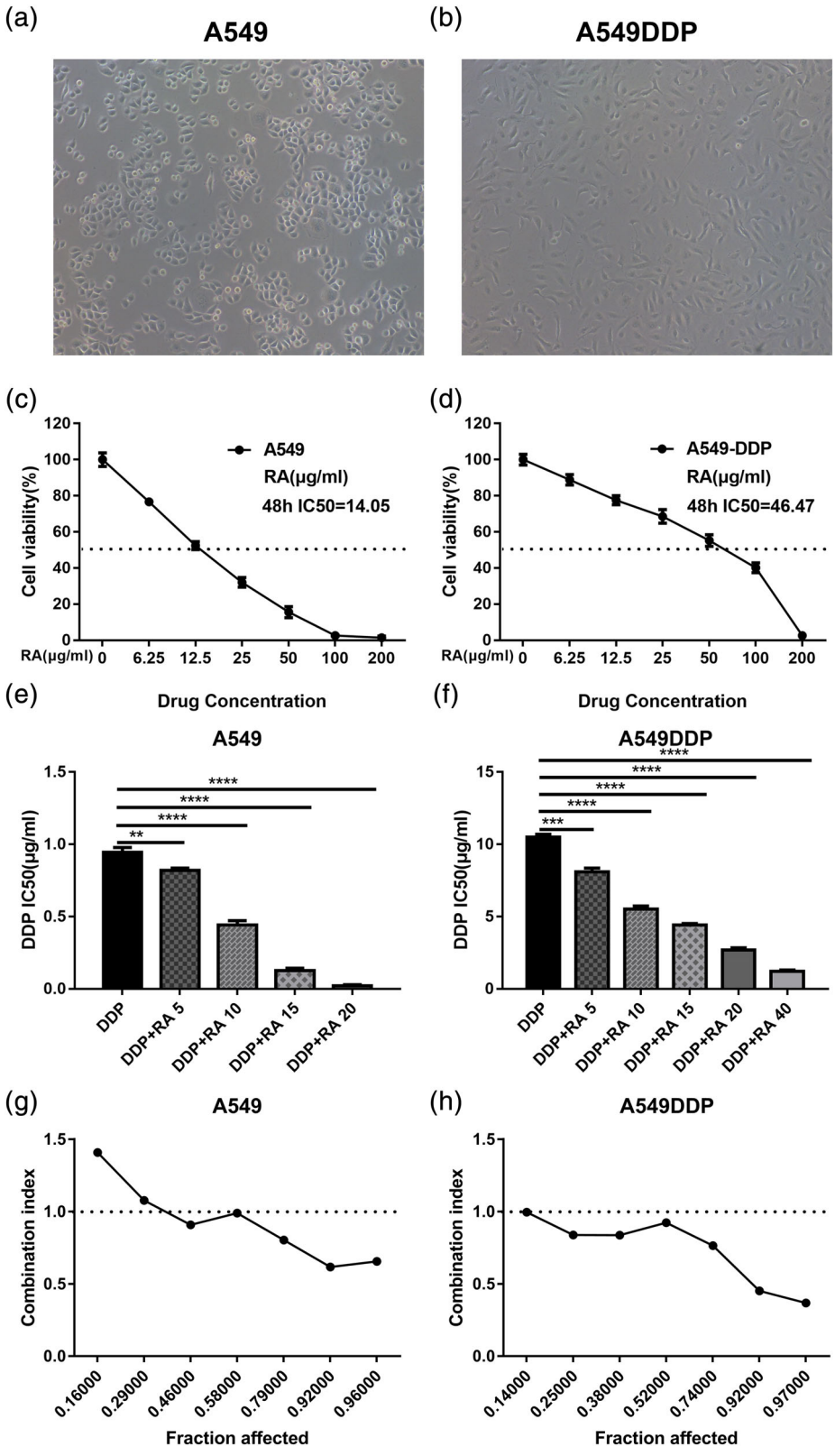

FIGURE 1 Inhibition of proliferation in NSCLC cell lines by RA. (a and b) Morphological changes of A549 cells undergoing cisplatin induced drug resistance. (c and d) Effects of RA on the growth of NSCLC cell lines, A549 and A549DDP. Cells were treated with various concentrations of RA for 48 hr and cell viability was measured by CCK8 assay. (e and f) The effects of 48 hr treatment with DDP and DDP combined with various concentrations of RA on the growth of A549 and A549DDP cells. The half maximal inhibitory concentration (IC_{50}) was quantified. (g and h) The combination index (CI) of RA and DDP in A549 and A549DDP was below 1. All data are presented as the mean ± *SD* of three independent experiments. $^{**}p < .01$; $^{***}p < .001$ compared to the control. DDP, cisplatin; NSCLC, non-small cell lung cancer; RA, rosmarinic acid [Colour figure can be viewed at wileyonlinelibrary.com]

inhibited cell proliferation in a dose-dependent manner in NSCLC cell lines, with IC_{50} values of 14.05 μg/ml in A549 cells and 46.47 μg/ml in A549DDP cells. We also found that under combined RA and DDP treatment, the sensitivity of NSCLC cells to DDP significantly increased (Figure 1e,f; Figure S1c,d). Our results also showed that the CI of RA and DDP in A549 and A549/DDP was below 1 (Figure 1g,h), indicating that the combination of RA and DDP showed synergistic effects.

Next, the CCK8 method was used to analyze the toxicity of RA and DDP in human normal somatic cells, namely, human bronchial epithelial cells (BEAS-2B). As shown in Figure S1g,h, the IC_{50} of RA against BEAS-2B cells was significantly higher than that against NSCLC cell lines. The reduced toxicity of RA to normal cells suggests that it could be used as a potential agent for reversing NSCLC cisplatin resistance.

4.2 | RA inhibits cell proliferation and induces cell cycle arrest in both A549 and A549DDP cell lines

Moreover, compared with untreated controls and the DDP-treated cells, RA and DDP combined treatment inhibited cell proliferation in a dose-dependent manner in A549 and A549DDP cells (Figure 2a,b). Inhibition of cell proliferation is associated with cell cycle, and thus, we examined the effect of RA combined with DDP on cell cycle progression in NSCLC cells. The results showed that cell cycle was arrested at the G1 phase when NSCLC cells were treated with RA for 48 hr, compared with untreated control and the DDP positive control cells (Figure 2c,d). In addition, the cycle arrest induced by RA showed dose dependence. To explore the mechanism of cell cycle arrest, we investigated the expression of cell cycle-related proteins, including p53 and p21. As shown in Figure 2e,f, RA combined with DDP treatment at different concentrations caused an increase in p53 and p21 expression in NSCLC cell lines. These results illustrate that RA combined with DDP can inhibit NSCLC cell proliferation and induce cell cycle arrest.

4.3 | RA combined with DDP increased apoptosis in A549 and A549DDP cells

Next, we examined the effect of RA and the combination therapy on NSCLC cells, which were treated with DDP alone or in combination with RA for 48 hr. As shown in Figure 3a,b, treatment with RA increased DDP-induced NSCLC cell apoptosis in a dose-dependent manner. Then, we investigated the effects of RA on apoptosis-related proteins, and the results showed that RA significantly increased cleaved Caspase-3 and Bax levels, but suppressed antiapoptotic Bcl-2 and Caspase-3 expression, which was consistent with the obvious upregulation of p53 (Figure 2e,f).

Moreover, RA combined with DDP enhanced the protein levels of cleaved caspase-3 in both the A549 and A549DDP cell lines in a dose-dependent manner (Figure 3c,d). Taken together, our results indicate that RA combined with DDP can induce mitochondria-mediated apoptosis and caspase activation in A549 and A549DDP cells.

4.4 | RA induced a dose-dependent reduction in P-gp-mediated drug resistance in NSCLC and in resistant NSCLC cell lines

To verify the drug resistance mechanism of A549DDP cells, RT-PCR and western blotting were used to quantify MDR1 mRNA and P-gp protein levels, respectively (Figure 4a–f). Compared with the parental A549 cell line, MDR1 gene expression and P-gp protein expression were significantly higher in the resistant A549DDP cell line. When both cell lines were treated with DDP, MDR1 mRNA, and P-gp protein expression levels were significantly upregulated. These results suggest that the mechanism that confers DDP resistance to A549 cells involves upregulation of MDR1 mRNA and P-gp protein expression, leading to increased drug efflux and a reduction in intracellular drug accumulation.

With an increase in RA concentration, the MDR1 expression levels were significantly reduced, and downregulation of P-gp contributed to RA-induced apoptosis, indicating that RA could be used as an MDR-mediated NSCLC DDP resistance reversal agent.

4.5 | Potential RA target proteins and KEGG pathway analysis

Using Pharma Mapper, we obtained information about the top 300 potential protein targets for RA (Table S1), and then, KEGG pathway analysis reminded us that RA might primarily influence the MAPK signaling pathway, as shown in Figure 5a,b.

Furthermore, much experimental evidence has shown that JNK, a member of the MAPK family, is closely related to the occurrence of MDR (Zhang et al., 2016). To explore the mechanisms underlying the antitumor and resistance reversal activity of RA, we determined the effects of RA on JNK activity. As shown in Figure 5c–f, RA increased the expression and activation of JNK, and we blocked the MAPK signaling pathway through JNK chemical inhibitor (SP600125), and the active effect of combination therapy on MAPK signaling pathway was partially recovered.

Mechanistically, RA inhibited NSCLC cell growth, induced apoptosis by activating phosphorylation of JNK and consequently reduced P-gp expression, which led to reversal of P-gp-mediated DDP resistance and promotion of mitochondria-mediated apoptosis.

4.6 | RA combined with DDP inhibited NSCLC xenograft tumor growth

We also inspected the effect of RA on the growth of xenograft NSCLC tumors. The experimental setup, including NSCLC cell

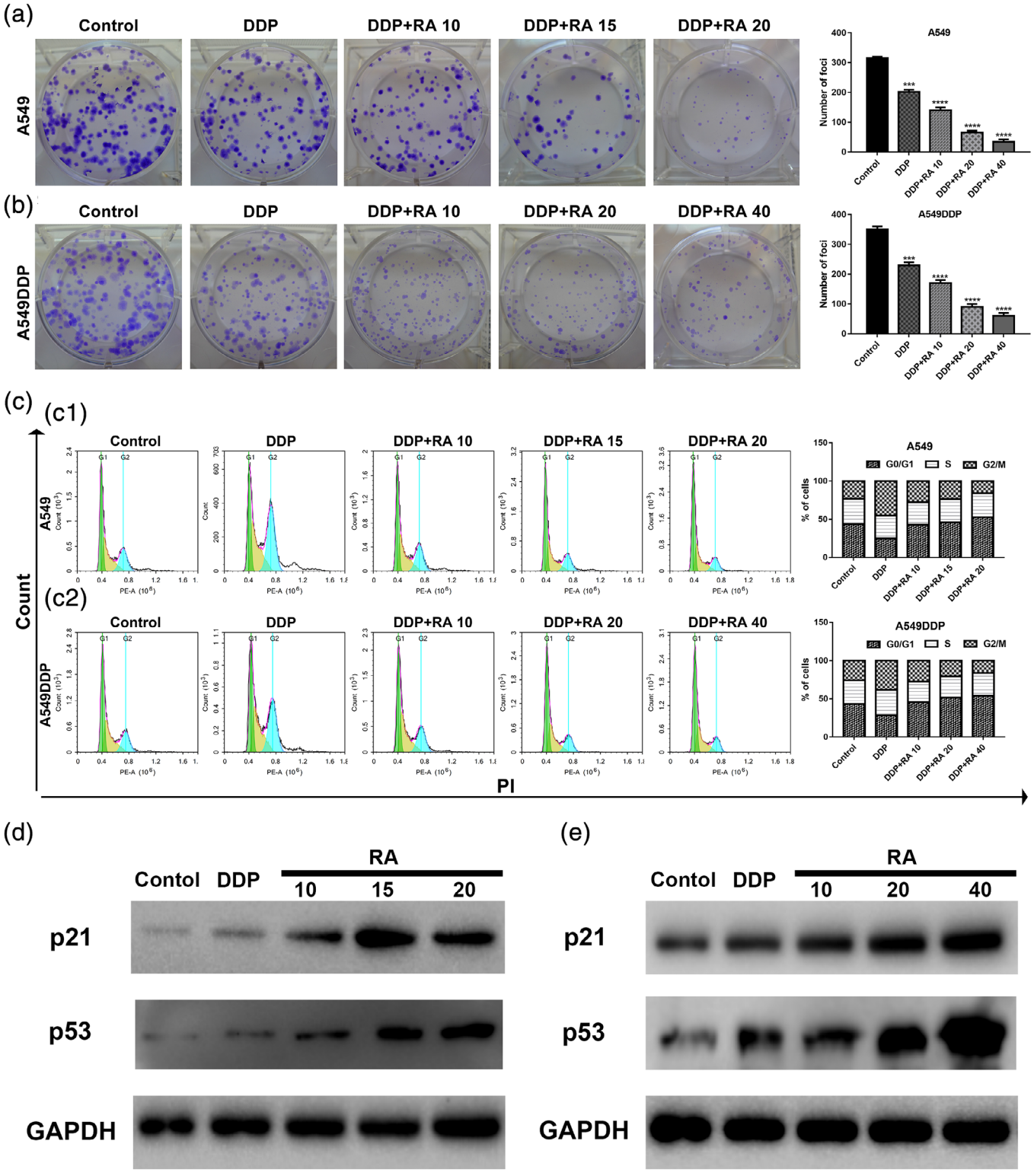

FIGURE 2 Inhibition of cell proliferation and induction of cell cycle arrest by DDP alone and combined with RA in NSCLC cell lines. (a and b) Cells were treated with 0, 10, 15, 20, and 40 μg/ml RA combined with 1.5 or 15 μg/ml DDP for 48 hr; representative images of A549 (a) and A549DDP (b) clone formation are shown. ***$p < .001$ compared with the control. (c and d) Cell cycle analysis. Percentages of A549 and A549DDP cells in the G1, S, and G2/M phases are presented, respectively. Effects of DDP and combined with various concentrations of RA medication on cell cycle distribution. A549 (c) and A549DDP (d) cells were treated with 0, 10, 15, 20, and 40 μg/ml RA combined with DDP for 48 hr, and cell cycle distribution was measured by flow cytometry after PI staining. (e and f) p21 and p53 protein levels were determined by western blot analyses. GAPDH was used as the loading control. DDP, cisplatin; NSCLC, non-small cell lung cancer; PI, propidium iodide; RA, rosmarinic acid [Colour figure can be viewed at wileyonlinelibrary.com]

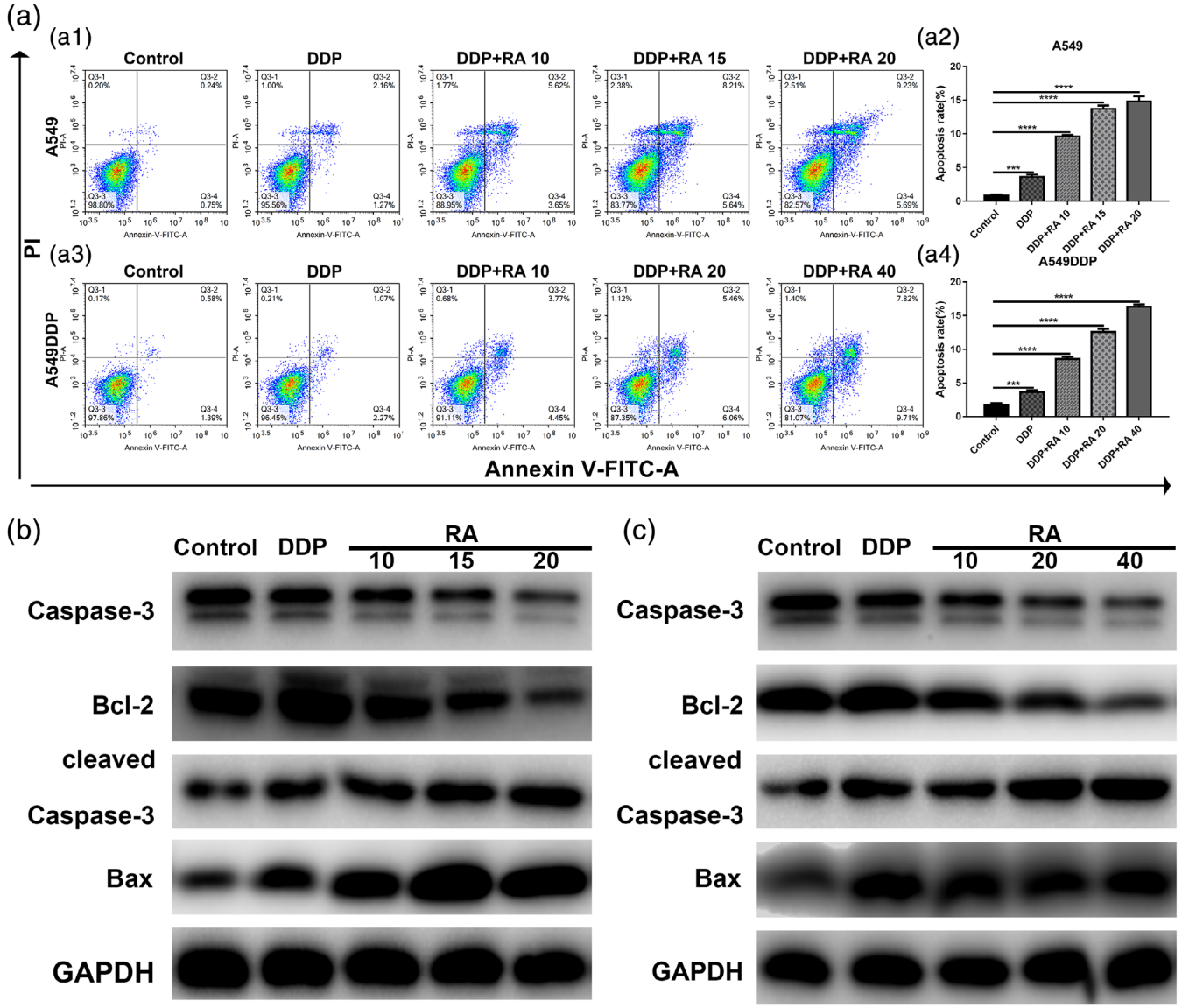

FIGURE 3 Induction of cell apoptosis by RA in NSCLC cell lines. (a1–a4) Induction of apoptosis by 1.5 or 15 μg/ml DDP and DDP combined with various concentrations of RA in A549 (a1, a2) and A549DDP (a3, a4) cells evaluated by Annexin-V-FITC/PI staining. (b) Western blot analysis of Bcl-2, Bax, Caspase-3 and cleaved Caspase-3. A549 cells were treated with DDP and combined with various concentrations of RA medication for 48 hr. GAPDH was used as the loading control. (c) Western blot analysis of Bcl-2, Bax, Caspase-3 and cleaved Caspase-3. A549 cells were treated with DDP and combined with various concentrations of RA medication for 48 hr. GAPDH was used as the loading control. $^{**}p < 0.01$; $^{***}p < 0.001$; versus control. DDP, cisplatin; NSCLC, non-small cell lung cancer; PI, propidium iodide; RA, rosmarinic acid [Colour figure can be viewed at wileyonlinelibrary.com]

inoculation and drug treatment, is shown in Figure 6a. In the control group, xenograft tumors grew faster and the tumor volume was significantly higher than in the RA-treated group (Figure 6c,e,g,h). However, RA treatment did not affect the body weight of the nude mice compared with that of mice in the control group. These results demonstrate that RA did not affect the health of the mice (Figure 6b). Our data suggest that DDP combined with RA can significantly inhibit tumor growth compared with DDP alone.

This work clearly revealed that combination therapy with DDP and RA had a synergistic cytotoxic effect on NSCLC and stimulated apoptosis through downregulation of antiapoptotic Bcl-2 expression, upregulation of p21 and p53 expression, activation of the JNK signaling pathway, inhibition of P-gp expression, and reduction of DDP efflux from NSCLC cells to increase DDP accumulation in tumor cells and increase tumor cell sensitivity to DDP. Finally, RA led to reversal of MDR in NSCLC via activation of the JNK signaling pathway, suggesting that RA may be a novel drug for clinical cancer chemotherapy treatment in the future.

5 | DISCUSSION

Lung cancer is a leading cause of global cancer-related death for both men and women. NSCLC accounts for approximately 85% of lung

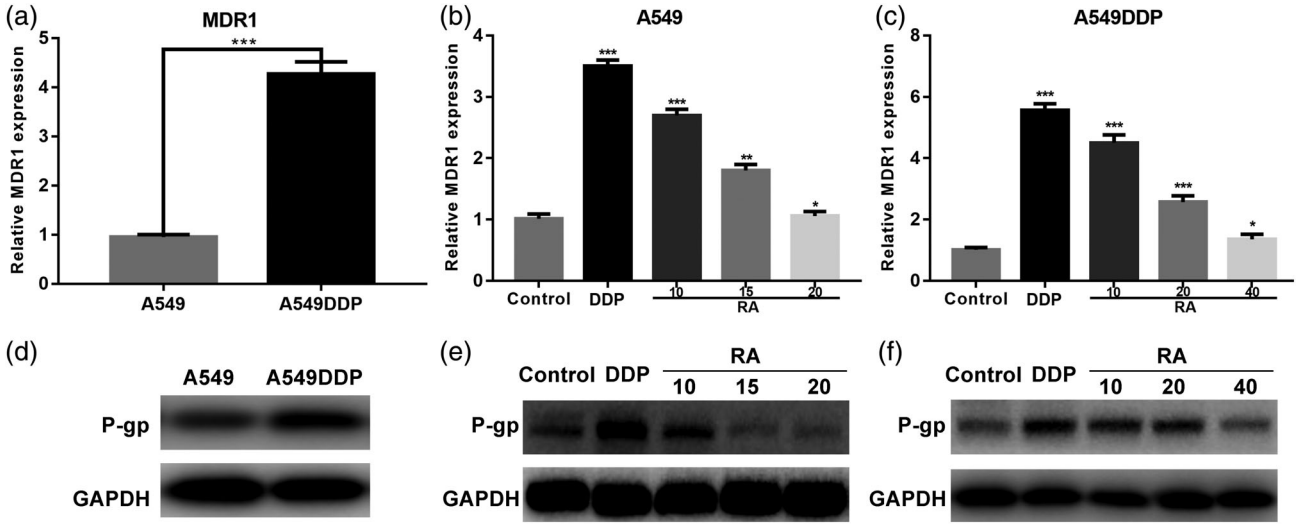

FIGURE 4 RA dose-dependent reduction of p-gp mediated drug resistance in NSCLC cell lines. (a) Relative expression of *MDR1* mRNA was examined by qRT-PCR in A549 cells and A549DDP cells. Expression of the housekeeping gene GAPDH was used as reference. (b and c) Relative expression of *MDR1* mRNA was examined by qRT-PCR in A549 cells and A549DDP cells in the presence or absence of RA under DDP conditions. Expression of the housekeeping gene GAPDH was used as reference. (d–f) Western blotting detection of P-gp protein expression in A549 and A549DDP cells treated with DDP and DDP combined with various concentrations of RA for 48 hr. GAPDH was used as the internal loading control. Data are presented as mean ± *SD* of three independent experiments. ***$p < .01$ versus control. DDP, cisplatin; NSCLC, non-small cell lung cancer; RA, rosmarinic acid

cancer cases (Siegel, Miller, & Jemal, 2017). Currently, in clinical therapy, most anticancer agents kill cells by interfering with DNA replication or by inducing DNA damage, which in turn leads to cell apoptosis (Gottesman, 2002; Liu, 2009). Among these anticancer drugs, cisplatin represents a successful landmark in the history of cancer clinical therapy. Once taken into cells, cisplatin intercalates, and forms intrastrand crosslinks in DNA, interferes with DNA replication and induces DNA damage, eventually triggering apoptosis or necrosis. Cisplatin-based doublets are widely used for NSCLC treatment and improve survival rates compared with placebo treatment (Rajeswaran, Trojan, Burnand, & Giannelli, 2008). However, the most important problem related to NSCLC therapy is intrinsic resistance to chemotherapeutics (Cruz-Bermudez et al., 2019). The mechanisms of cisplatin resistance require further elucidation. Hence, profound discovery and understanding of its mode of action may lead to new therapeutic regimens to overcome cisplatin resistance and improve the overall survival of patients with NSCLC. While research has made advances in the field of MDR, it remains a huge problem in clinical treatment.

The mechanism underlying resistance to chemotherapy is very complex; one of the main mechanisms is the P-gp-mediated increase in efflux of drugs (Galluzzi et al., 2012). P-gp belongs to the ABC transporter superfamily, which includes the main drug efflux transporters associated with chemotherapy failure in cancer (Chen et al., 2016). Much attention has been paid to the molecular mechanisms that regulate the expression of these transporters as a viable approach to identify novel drug targets to circumvent MDR clinically (Juliano & Ling, 1976; Levatic et al., 2013; S. Li et al., 2015). In our study, we constructed an in vitro MDR model, the A549DDP cell line, which was 10-fold more resistant to DDP than the parental A549 cell line. In this cell line, MDR1 gene expression was significantly higher, and therefore, we used it to study the role of RA in MDR.

Natural bioactive products are a rich source of novel therapeutics derived from plentiful natural substances, such as plants, fruits, and mushrooms. Numerous researchers have focused on natural extracts owing to the success of artemisinin (qinghaosu; Kumari et al., 2019) and arsenic (III) oxide (As_2O_3) (Kaiming et al., 2018) in the clinic. Given their safety, long-term use, and ability to target multiple pathways, there is renewed interest in understanding the molecular mechanisms underlying their activity. Small molecules extracted from Chinese herbal medicine were reported in the literature to be able to reverse MDR in malignant tumors (Ahmed, Hassan, & Kondo, 2015; Deferme, Van Gelder, & Augustijns, 2002). RA, one of the most important and well known natural antioxidant compounds, is produced by the rosemary plant in the Lamiaceae family. Some reports have provided evidence that RA has therapeutic potential for many diseases, and side effects of RA have rarely been reported (Nabavi et al., 2015). Among the many biological activities of RA, more attention has been paid to its ability to increase the sensitivity of tumor cells to chemotherapeutic drugs (Huang, Cai, Huang, & Zheng, 2018; Sengelen & Onay-Ucar, 2018; Yu et al., 2019). These findings suggest that RA has potential as a novel adjunct to chemotherapy.

Although RA has been used as an antitumor agent and MDR reversal agent in different types of cancers and one of the identified anti-MDR mechanisms is inhibition of P-gp expression and function, the antitumor effect of RA and whether it can reverse MDR in NSCLC remain largely unknown. Therefore, in this study, we examined the potential antitumor and drug resistance reversal activity of RA. We found that RA did not affect the proliferation of

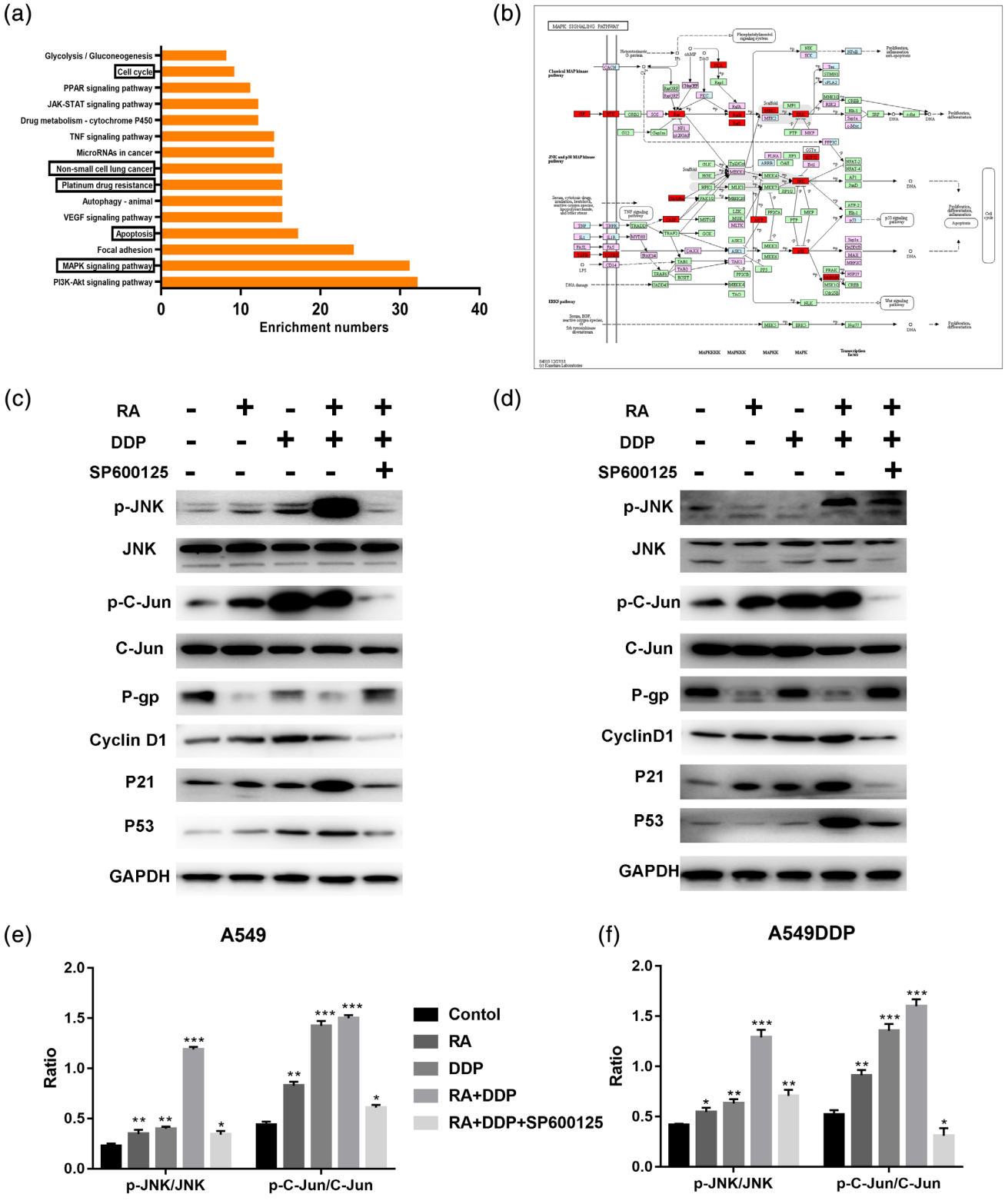

FIGURE 5 KEGG pathway analysis of Tan IIA and the MAPK signaling pathway. (a) The top 15 signaling pathways of Tan IIA in KEGG pathway analysis. (b) The MAPK signaling pathway and the potential target protein (red) of RA. (c and d) A549 and A549DDP cells were treated for 48 hr with RA, DDP, or SP600125, western blotting detection of JNK, p-JNK, Jun, p-c-Jun, P-gp, Cyclin D1, P21, and P53 proteins. GAPDH was used as an internal control. Data are presented as mean ± *SD* of three independent experiments. ***$p < .01$ versus control. DDP, cisplatin; RA, rosmarinic acid [Colour figure can be viewed at wileyonlinelibrary.com]

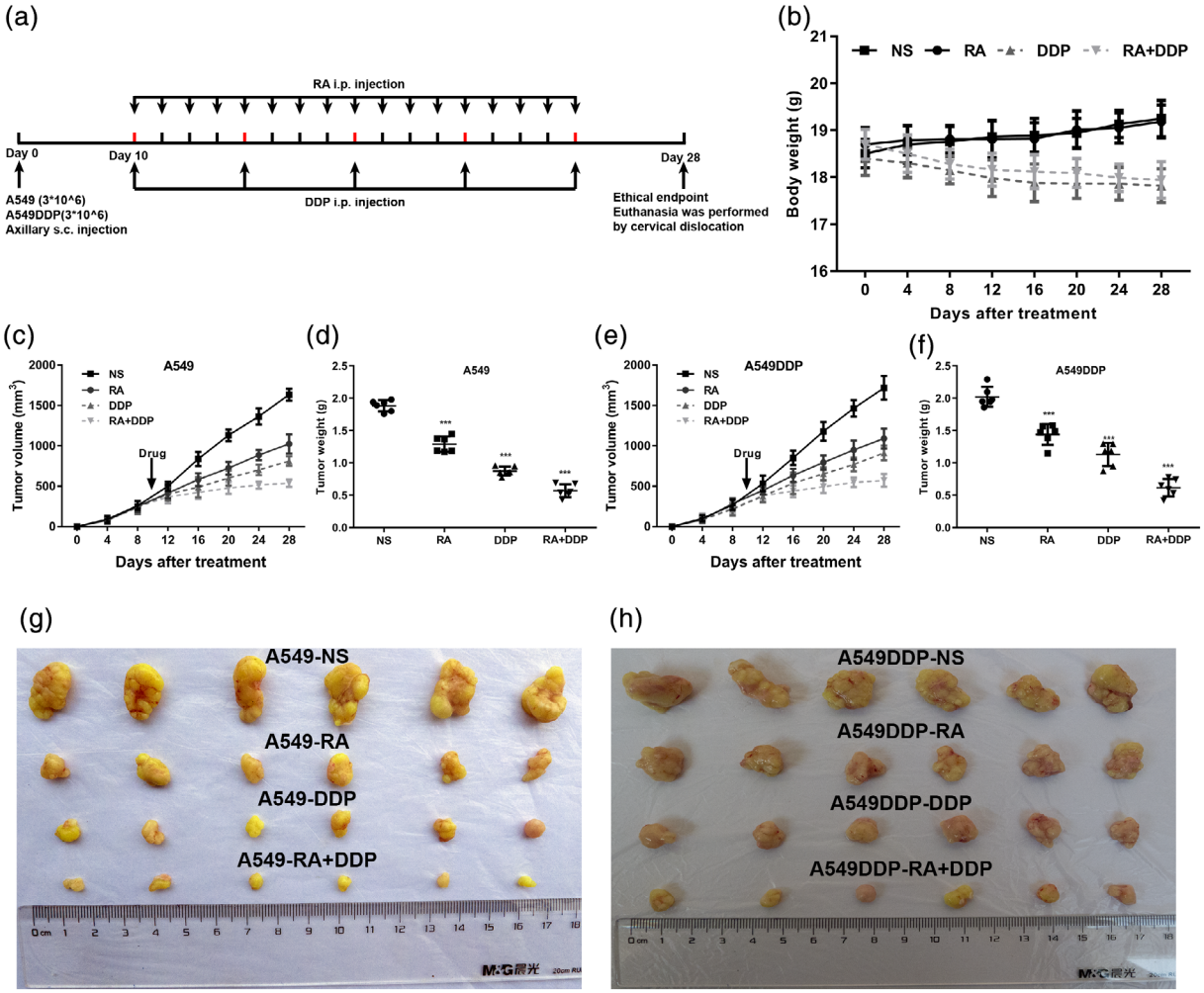

FIGURE 6 RA combined with DDP inhibits NSCLC xenograft tumor growth. (a) Timeline of NSCLC cell inoculation and drug treatment. (b) Time courses of animal weight. (c) Time courses of A54 cells xenograft tumor growth. (d) Dots graphs represent the weight of the A549 cells xenograft tumor after various treatments. (e) Time courses of A549DDP cells xenograft tumor growth were measured in each group at the indicated time point of various treatments. (f) Dots graphs represent the weight of the A549DDP xenograft tumor after various treatments. (g and h) Visual comparison of the dissected tumor tissues. Representative pictures of tumor growth in mice treated with vehicle control and the various treatments are shown. Data are presented as mean ± *SD*. $^{**}p < .01$; $^{***}p < .001$. $N = 5$ in each group. DDP, cisplatin; NSCLC, non-small cell lung cancer; RA, rosmarinic acid [Colour figure can be viewed at wileyonlinelibrary.com]

normal cells up to a concentration of 14.05 μg/ml; the IC_{50} value was 29.52 μg/ml. Furthermore, we analyzed the synergy (CI < 1) of RA combined with DDP using the CalcuSyn software (Ashton, 2015) and found that the combination of RA and DDP met the sensitized and attenuated principle. Huang et al. reported that RA had a direct cytotoxic effect on HepG2 and Bel-7,402 human liver carcinoma cells (Huang et al., 2018). Similarly, we found that RA could inhibit the growth of A549 and A549DDP NSCLC cell lines, and the antineoplastic activity showed concentration dependence.

Recent studies have demonstrated that RA treatment results in an increased apoptosis rate in gastric cancer (W. Li et al., 2019) and could reverse the MDR in gastric cancer (F. R. Li et al., 2013). We examined the Bcl-2-Bax signaling pathway and confirmed that RA combined with DDP could significantly downregulate the expression of Bcl-2 in A549 and A549DDP cells. This result demonstrates that RA can reverse MDR in NSCLC by modulating complex signal transduction.

Recent evidence has indicated that JNK regulates MDR1 expression (Bark & Choi, 2010). JNK regulates a series of cellular biological processes, including expression of the MDR1 gene, through c-Jun-transmitted signals (Bark & Choi, 2010; Cerezo et al., 2017). In addition, using PharmaMapper (Wang et al., 2017) and KEGG pathway analysis, we found that RA might primarily influence the MAPK signaling pathway. However, little is known about how RA reverses MDR by regulating P-gp expression through the JNK/c-Jun signaling pathway. Therefore, we focused on JNK/c-Jun as a target to investigate the mechanism by which RA reverses MDR in NSCLC cells.

Inactivation of the p53 tumor suppressor gene occurs in over half of all human tumors, implying that loss of this gene represents a fundamentally important step in the pathogenesis of cancer. p53 might

cause cell cycle arrest through the transactivation of p21, and this pathway might inhibit cell growth and activate the apoptotic pathway by cytochrome c release and caspase activation. Our data demonstrated that RA induced a dose-dependent upregulation of p53 and the downstream p21, explaining the mechanism by which RA can caused cell cycle arrest, inhibited proliferation, and induced apoptosis.

In NSCLC xenograft models, we discovered that RA increased the sensitivity of NSCLC to DDP. RA or DDP alone could play a role in inhibiting NSCLC growth in vivo. However, combined treatment with RA and DDP significantly enhanced the inhibition of growth compared with the DDP monotherapy group. The antitumor effect was dependent on the concentration of RA, and 10 mg/kg RA combined with DDP had the strongest inhibitory effect on NSCLC. Similar to the in vitro results, RA reversed DDP resistance in NSCLC in vivo.

In summary, our study demonstrates that RA can effectively reverse MDR-mediated cisplatin resistance in NSCLC cells in vitro and in vivo, induce significant apoptosis in the human A549 NSCLC cell line and its resistant strain A549DDP, inhibit NSCLC cell proliferation, and induce G1 phase cell cycle arrest. This study demonstrates the central importance of RA in DDP resistance reversal in NSCLC, and the collective findings show a mechanistic link between RA and JNK signaling, indicating that RA is a potential therapeutic agent for NSCLC resistance. Thus, this study provides evidence for further research and development of this drug for cancer chemotherapy.

ACKNOWLEDGMENTS

We would like to thank the Sun Yat-sen University Cancer Center for providing facilities and support throughout our research. Great thanks are extended to Ying He, Kai Qin, and Zi-Hao Feng for their vital direction and crucial help in the research process.

CONFLICT OF INTEREST

The authors declare that they have no competing interests.

AUTHOR CONTRIBUTIONS

L.Z.L. and W.H.C. conceived and designed the study. X.Z.L., Y.G., and L.L.S. performed the in vitro and in vivo experiments and analyzed the data. X.Z.L. wrote the manuscript. J.H.L., L.L.S., H.R.C., L.Y., and Z.Z.C. helped revise the manuscript. L.Z.L. and W.H.C. revised the manuscript. All the authors read and approved the final manuscript.

CONSENT FOR PUBLICATION

Consent to publish has been obtained from all authors.

ETHICS APPROVAL AND CONSENT TO PARTICIPATE

All aspects of this study were approved by the medical ethics committee of Sun Yat-Sen University Cancer Center. All animal studies were performed with approval from the Institutional Animal Care and Use Committee of Sun Yat-Sen University.

DATA AVAILABILITY STATEMENT

All data generated or analyzed during this study are included in this published article.

ORCID

Li-Zhu Lin https://orcid.org/0000-0001-8283-6554

REFERENCES

Abdallah, H. M., Al-Abd, A. M., El-Dine, R. S., & El-Halawany, A. M. (2015). P-glycoprotein inhibitors of natural origin as potential tumor chemosensitizers: A review. *Journal of Advanced Research*, *6*(1), 45–62. https://doi.org/10.1016/j.jare.2014.11.008

Ahmed, I. S., Hassan, M. A., & Kondo, T. (2015). Effect of lyophilized grapefruit juice on P-glycoprotein-mediated drug transport in-vitro and in-vivo. *Drug Development and Industrial Pharmacy*, *41*(3), 375–381. https://doi.org/10.3109/03639045.2013.866141

Alakhova, D. Y., & Kabanov, A. V. (2014). Pluronics and MDR reversal: An update. *Molecular Pharmaceutics*, *11*(8), 2566–2578. https://doi.org/10.1021/mp500298q

Ashton, J. C. (2015). Drug combination studies and their synergy quantification using the Chou-Talalay method—letter. *Cancer Research*, *75*(11), 2400. https://doi.org/10.1158/0008-5472.can-14-3763

Bark, H., & Choi, C. H. (2010). PSC833, cyclosporine analogue, down-regulates MDR1 expression by activating JNK/c-Jun/AP-1 and suppressing NF-kappaB. *Cancer Chemotherapy and Pharmacology*, *65*(6), 1131–1136. https://doi.org/10.1007/s00280-009-1121-7

Cerezo, D., Ruiz-Alcaraz, A. J., Lencina-Guardiola, M., Canovas, M., Garcia-Penarrubia, P., Martinez-Lopez, I., & Martin-Orozco, E. (2017). Attenuated JNK signaling in multidrug-resistant leukemic cells. Dual role of MAPK in cell survival. *Cellular Signalling*, *30*, 162–170. https://doi.org/10.1016/j.cellsig.2016.12.003

Chen, Z., Shi, T., Zhang, L., Zhu, P., Deng, M., Huang, C., … Li, J. (2016). Mammalian drug efflux transporters of the ATP binding cassette (ABC) family in multidrug resistance: A review of the past decade. *Cancer Letters*, *370*(1), 153–164. https://doi.org/10.1016/j.canlet.2015.10.010

Choi, Y. H., & Yu, A. M. (2014). ABC transporters in multidrug resistance and pharmacokinetics, and strategies for drug development. *Current Pharmaceutical Design*, *20*(5), 793–807.

Cruz-Bermudez, A., Laza-Briviesca, R., Vicente-Blanco, R. J., Garcia-Grande, A., Coronado, M. J., Laine-Menendez, S., … Provencio, M. (2019). Cisplatin resistance involves a metabolic reprogramming through ROS and PGC-1alpha in NSCLC which can be overcome by OXPHOS inhibition. *Free Radical Biology & Medicine*, *135*, 167–181. https://doi.org/10.1016/j.freeradbiomed.2019.03.009

Deferme, S., Van Gelder, J., & Augustijns, P. (2002). Inhibitory effect of fruit extracts on P-glycoprotein-related efflux carriers: An in-vitro screening. *The Journal of Pharmacy and Pharmacology*, *54*(9), 1213–1219. https://doi.org/10.1211/002235702320402053

Fennell, D. A., Summers, Y., Cadranel, J., Benepal, T., Christoph, D. C., Lal, R., … Ferry, D. (2016). Cisplatin in the modern era: The backbone of first-line chemotherapy for non-small cell lung cancer. *Cancer Treatment Reviews*, *44*, 42–50. https://doi.org/10.1016/j.ctrv.2016.01.003

Ferlay, J., Soerjomataram, I., Dikshit, R., Eser, S., Mathers, C., Rebelo, M., … Bray, F. (2015). Cancer incidence and mortality worldwide: Sources, methods and major patterns in GLOBOCAN 2012. *International Journal of Cancer*, *136*(5), E359–E386. https://doi.org/10.1002/ijc.29210

Galluzzi, L., Senovilla, L., Vitale, I., Michels, J., Martins, I., Kepp, O., … Kroemer, G. (2012). Molecular mechanisms of cisplatin resistance. *Oncogene*, *31*(15), 1869–1883. https://doi.org/10.1038/onc.2011.384

Gottesman, M. M. (2002). Mechanisms of cancer drug resistance. *Annual Review of Medicine*, *53*, 615–627. https://doi.org/10.1146/annurev.med.53.082901.103929

Gottesman, M. M., & Pastan, I. H. (2015). The role of multidrug resistance efflux pumps in cancer: Revisiting a JNCI publication exploring expression of the MDR1 (P-glycoprotein) Gene. *Journal of the National Cancer Institute*, *107*(9), djv222. https://doi.org/10.1093/jnci/djv222

Gutierrez-Grijalva, E. P., Picos-Salas, M. A., Leyva-Lopez, N., Criollo-Mendoza, M. S., Vazquez-Olivo, G., & Heredia, J. B. (2017). Flavonoids

and phenolic acids from oregano: Occurrence, biological activity and health benefits. *Plants (Basel)*, *7*(1). https://doi.org/10.3390/plants7010002

Han, S., Yang, S., Cai, Z., Pan, D., Li, Z., Huang, Z., … Wang, W. (2015). Anti-Warburg effect of rosmarinic acid via miR-155 in gastric cancer cells. *Drug Design, Development and Therapy*, *9*, 2695–2703. https://doi.org/10.2147/dddt.s82342

Huang, Y., Cai, Y., Huang, R., & Zheng, X. (2018). Rosmarinic acid combined with Adriamycin induces apoptosis by triggering mitochondria-mediated signaling pathway in HepG2 and Bel-7402 cells. *Medical Science Monitor*, *24*, 7898–7908. https://doi.org/10.12659/msm.910673

Juliano, R. L., & Ling, V. (1976). A surface glycoprotein modulating drug permeability in Chinese hamster ovary cell mutants. *Biochimica et Biophysica Acta*, *455*(1), 152–162.

Kaiming, C., Sheng, Y., Zheng, S., Yuan, S., Huang, G., & Liu, Y. (2018). Arsenic trioxide preferentially binds to the ring finger protein PML: Understanding target selection of the drug. *Metallomics*, *10*(11), 1564–1569. https://doi.org/10.1039/c8mt00202a

Kim, G. D., Park, Y. S., Jin, Y. H., & Park, C. S. (2015). Production and applications of rosmarinic acid and structurally related compounds. *Applied Microbiology and Biotechnology*, *99*(5), 2083–2092. https://doi.org/10.1007/s00253-015-6395-6

Kumari, A., Karnatak, M., Singh, D., Shankar, R., Jat, J. L., Sharma, S., … Verma, V. P. (2019). Current scenario of artemisinin and its analogues for antimalarial activity. *European Journal of Medicinal Chemistry*, *163*, 804–829. https://doi.org/10.1016/j.ejmech.2018.12.007

Levatic, J., Curak, J., Kralj, M., Smuc, T., Osmak, M., & Supek, F. (2013). Accurate models for P-gp drug recognition induced from a cancer cell line cytotoxicity screen. *Journal of Medicinal Chemistry*, *56*(14), 5691–5708. https://doi.org/10.1021/jm400328s

Li, F. R., Fu, Y. Y., Jiang, D. H., Wu, Z., Zhou, Y. J., Guo, L., … Wang, Z. Z. (2013). Reversal effect of rosmarinic acid on multidrug resistance in SGC7901/Adr cell. *Journal of Asian Natural Products Research*, *15*(3), 276–285. https://doi.org/10.1080/10286020.2012.762910

Li, S., Zhang, W., Yin, X., Xing, S., Xie, H. Q., Cao, Z., & Zhao, B. (2015). Mouse ATP-binding cassette (ABC) transporters conferring multi-drug resistance. *Anti-Cancer Agents in Medicinal Chemistry*, *15*(4), 423–432.

Li, W., Li, Q., Wei, L., Pan, X., Huang, D., Gan, J., & Tang, S. (2019). Rosmarinic acid analogue-11 induces apoptosis of human gastric cancer SGC-7901 cells via the epidermal growth factor receptor (EGFR)/Akt/nuclear factor kappa B (NF-kappaB) pathway. *Medical Science Monitor Basic Research*, *25*, 63–75. https://doi.org/10.12659/msmbr.913331

Liu, F. S. (2009). Mechanisms of chemotherapeutic drug resistance in cancer therapy—A quick review. *Taiwanese Journal of Obstetrics & Gynecology*, *48*(3), 239–244. https://doi.org/10.1016/s1028-4559(09)60296-5

Nabavi, S. F., Tenore, G. C., Daglia, M., Tundis, R., Loizzo, M. R., & Nabavi, S. M. (2015). The cellular protective effects of rosmarinic acid: From bench to bedside. *Current Neurovascular Research*, *12*(1), 98–105.

Pluchino, K. M., Hall, M. D., Goldsborough, A. S., Callaghan, R., & Gottesman, M. M. (2012). Collateral sensitivity as a strategy against cancer multidrug resistance. *Drug Resistance Updates*, *15*(1–2), 98–105. https://doi.org/10.1016/j.drup.2012.03.002

Rajeswaran, A., Trojan, A., Burnand, B., & Giannelli, M. (2008). Efficacy and side effects of cisplatin- and carboplatin-based doublet chemotherapeutic regimens versus non-platinum-based doublet chemotherapeutic regimens as first line treatment of metastatic non-small cell lung carcinoma: A systematic review of randomized controlled trials. *Lung Cancer*, *59*(1), 1–11. https://doi.org/10.1016/j.lungcan.2007.07.012

Reck, M., Popat, S., Reinmuth, N., De Ruysscher, D., Kerr, K. M., & Peters, S. (2014). Metastatic non-small-cell lung cancer (NSCLC): ESMO Clinical Practice Guidelines for diagnosis, treatment and follow-up. *Annals of Oncology*, *25*(Suppl 3), iii27–iii39. https://doi.org/10.1093/annonc/mdu199

Rocha, J., Eduardo-Figueira, M., Barateiro, A., Fernandes, A., Brites, D., Bronze, R., … Sepodes, B. (2015). Anti-inflammatory effect of rosmarinic acid and an extract of *Rosmarinus officinalis* in rat models of local and systemic inflammation. *Basic & Clinical Pharmacology & Toxicology*, *116*(5), 398–413. https://doi.org/10.1111/bcpt.12335

Rosell, R., Lord, R. V., Taron, M., & Reguart, N. (2002). DNA repair and cisplatin resistance in non-small-cell lung cancer. *Lung Cancer*, *38*(3), 217–227.

Schneider, E., Paul, D., Ivy, P., & Cowan, K. H. (1999). Multidrug resistance. *Cancer Chemotherapy and Biological Response Modifiers*, *18*, 152–177.

Sengelen, A., & Onay-Ucar, E. (2018). Rosmarinic acid and siRNA combined therapy represses Hsp27 (HSPB1) expression and induces apoptosis in human glioma cells. *Cell Stress & Chaperones*, *23*(5), 885–896. https://doi.org/10.1007/s12192-018-0896-z

Siegel, R. L., Miller, K. D., & Jemal, A. (2017). Cancer statistics, 2017. *CA: A Cancer Journal for Clinicians*, *67*(1), 7–30. https://doi.org/10.3322/caac.21387

Wang, X., Shen, Y., Wang, S., Li, S., Zhang, W., Liu, X., … Li, H. (2017). PharmMapper 2017 update: A web server for potential drug target identification with a comprehensive target pharmacophore database. *Nucleic Acids Research*, *45*(W1), W356–W360. https://doi.org/10.1093/nar/gkx374

Xia, Q., Wang, Z. Y., Li, H. Q., Diao, Y. T., Li, X. L., Cui, J., … Li, H. (2012). Reversion of p-glycoprotein-mediated multidrug resistance in human leukemic cell line by diallyl trisulfide. *Evidence-Based Complementary and Alternative Medicine*, *2012*, 719805–719811. https://doi.org/10.1155/2012/719805

Yu, C., Chen, D. Q., Liu, H. X., Li, W. B., Lu, J. W., & Feng, J. F. (2019). Rosmarinic acid reduces the resistance of gastric carcinoma cells to 5-fluorouracil by downregulating FOXO4-targeting miR-6785-5p. *Biomedicine & Pharmacotherapy*, *109*, 2327–2334. https://doi.org/10.1016/j.biopha.2018.10.061

Zhang, L., Zhang, Z., Chen, F., Chen, Y., Lin, Y., & Wang, J. (2016). Aromatic heterocyclic esters of podophyllotoxin exert anti-MDR activity in human leukemia K562/ADR cells via ROS/MAPK signaling pathways. *European Journal of Medicinal Chemistry*, *123*, 226–235. https://doi.org/10.1016/j.ejmech.2016.07.050

Zhou, S. F., Wang, L. L., Di, Y. M., Xue, C. C., Duan, W., Li, C. G., & Li, Y. (2008). Substrates and inhibitors of human multidrug resistance associated proteins and the implications in drug development. *Current Medicinal Chemistry*, *15*(20), 1981–2039.

Zhu, F., Asada, T., Sato, A., Koi, Y., Nishiwaki, H., & Tamura, H. (2014). Rosmarinic acid extract for antioxidant, antiallergic, and alpha-glucosidase inhibitory activities, isolated by supramolecular technique and solvent extraction from Perilla leaves. *Journal of Agricultural and Food Chemistry*, *62*(4), 885–892. https://doi.org/10.1021/jf404318j

SUPPORTING INFORMATION

Additional supporting information may be found online in the Supporting Information section at the end of this article.

How to cite this article: Liao X-Z, Gao Y, Sun L-L, et al. Rosmarinic acid reverses non-small cell lung cancer cisplatin resistance by activating the MAPK signaling pathway. *Phytotherapy Research*. 2020;34:1142–1153. https://doi.org/10.1002/ptr.6584